

# Annual Report 1998

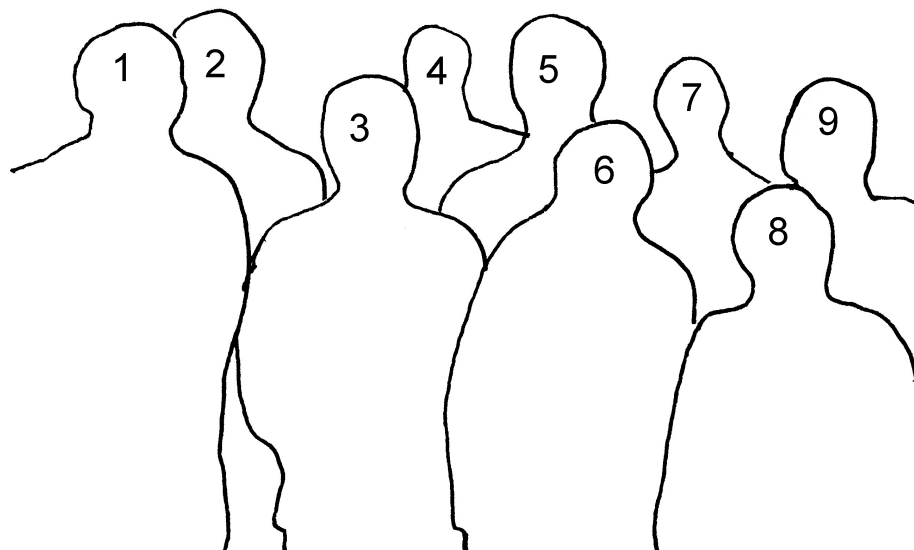


Chair of Optoelectronics  
Faculty of Mathematics and Computer Science  
University of Mannheim  
B6,26  
D - 68131 Mannheim  
Telephone +49 (0)621 / 292 - 5459  
Fax +49 (0)621 / 292 - 1605  
EMail [info@oe.ti.uni-mannheim.de](mailto:info@oe.ti.uni-mannheim.de)  
WWW <http://www.ti.uni-mannheim.de/~oe>

# **Contents**

<b>1 Members of the chair of Optoelectronics</b>	<b>2</b>
<b>2 Foreword</b>	<b>3</b>
<b>3 Projection Unit for optical 3D-Metrology based on Polarization Optics</b>	<b>4</b>
<b>4 Refractive Volume Holograms realized by Ion Exchange in Glass</b>	<b>5</b>
<b>5 Analysis of phase anomalies and design of continuous phase elements</b>	<b>6</b>
<b>6 Realization of planar microlenses with long focal distance by mask-synthesis</b>	<b>7</b>
<b>7 1:3 Beam-Splitting with a H-ROD Element</b>	<b>8</b>
<b>8 Variable Fractional Fourier Transform using an H-Rod Microlens</b>	<b>9</b>
<b>9 Experimental Characterization of Microoptical Objects in Phase Space</b>	<b>10</b>
<b>10 Angular Multiplexing for optical Board to Board Interconnections</b>	<b>11</b>
<b>11 Microobjectives with large numerical aperture by stacking of microlenses</b>	<b>12</b>
<b>12 Software Tools for Pattern Design in Lithography</b>	<b>13</b>
<b>13 Software for Computer Aided Surface Profiling</b>	<b>14</b>
<b>A List of recent Publications</b>	<b>15</b>

# 1 Members of the chair of Optoelectronics



1	Dr. Bähr Prof. Dr. Brenner	Jochen Karl-Heinz	1615 3004	jb@oe.ti.uni-mannheim.de brenner@rumms.uni-mannheim.de
2	Dengler	Christian		cdengler@rumms.uni-mannheim.de
3	Döringer	Oliver		doering@rumms.uni-mannheim.de
4	Dr. Dragoman	Daniela	1550	dd@oe.ti.uni-mannheim.de
5	Dr. Dragoman	Mircea	1613	md@oe.ti.uni-mannheim.de
6	Fauland	Michael		fauland@rumms.uni-mannheim.de
7	Flammuth	Sven		flammuth@rumms.uni-mannheim.de
8	Fröning	Holger		maddock@rumms.uni-mannheim.de
9	Klug	Robert	1613	rklug@oe.ti.uni-mannheim.de
	Dr. Krackhardt	Ulrich	5147	krackhdt@rumms.uni-mannheim.de
	Kraft	Michael	1616	kraft@oe.ti.uni-mannheim.de
	Oberhöffken	Arndt		wwwadmin@oe.ti.uni-mannheim.de
	Passon	Christoph	5541	c.passon@oe.ti.uni-mannheim.de
4	Reichel	Dirk		
	Schiek	Steffen		schiek@rumms.uni-mannheim.de
2	Schmelcher	Thilo	5541	t.schmelcher@oe.ti.uni-mannheim.de
9	Volk	Sabine	5459	office@oe.ti.uni-mannheim.de

## **2 Foreword**

*The last year has brought a few changes. Most importantly, since September, our chair is fortunate to have a new and highly efficient secretary, Mrs. Sabine Volk. If you have contacted me by telephone previously, you may have already made acquaintance with her kind voice. In the laboratory, our technician, Michael Kraft continues his excellent work, helping us to solve many of the technological problems. In February of last year, an old friend and well-known specialist for Wigner functions, Daniela Dragoman came as a Humboldt-visiting professor together with her husband, who is also a professor at the National Research Institute for Microtechnology in Bucharest, Romania. This visit has already created several productive results. So, our work on the hemispherical rod lens could be merged with the expertise of Daniela Dragoman on fractional Fourier-transforms and resulted in a joint publication. One of my PhD-Students, Christoph Passon has reached the end of his PhD-work and has left us. Thus his contributions to the annual report unfortunately could not be included here. For the design of continuous phase elements, after many years of search, now a satisfactory approach has been found, which is reported as contribution no. 3 in this report. Another new development, the angular multiplexing of signals in a multi-mode fiber has developed into a very promising technique for short distance interconnections. Our first students of computer engineering are now in their fifth semester and some of them have already used the opportunity of accepting short jobs for contributing to the research work, which is documented in the contributions 12 and 13.*

*Karl-Heinz Brenner*

### 3 Projection Unit for optical 3D-Metrology based on Polarization Optics

*U.W. Krackhardt, K.-H. Brenner*

In optical 3D-metrology (topometry) object shapes or surface profiles, respectively, are acquired for subsequent digital processing. A well-established technique for imaging 3D-metrology is fringe projection: A fringe pattern is projected onto an object under test. The pattern is observed by a camera from a different direction. Depth information of the object can be obtained from the local fringe displacement. For resolving the fringe displacement with high accuracy, phase sampling techniques like in interferometry (PSI) are applied. Thereby, the fringe pattern is laterally shifted (phase shift) by a fraction of a fringe period between subsequent exposures.

However, this technique suffers from an ambiguity by principle: Fringe displacements, i.e. lateral fringe shifts, can only be detected up to multiples of the fringe period resulting in relative data. Absolute data can be obtained either by coding the fringe number (e.g. by Gray codes) or by using multiple fringe periods comparable to multiple wavelength interferometry.

Consequently, for achieving accurate and absolute data it is desirable to have adjustable fringe periods and phases. For rapid data acquisition it is necessary that the phase shift of a fringe pattern is the same for all patterns with different periods. We developed a fringe projection unit for measuring absolute data with no extra acquisition time in contrast to other absolute measurements [13]. The projection unit provides fringe patterns generated by interference. The optical set up is basically a polarization interferometer of the Michelson-type. The intensity distribution at the output of the interferometer is the fringe pattern. The period can be adjusted by tilting one mirror.

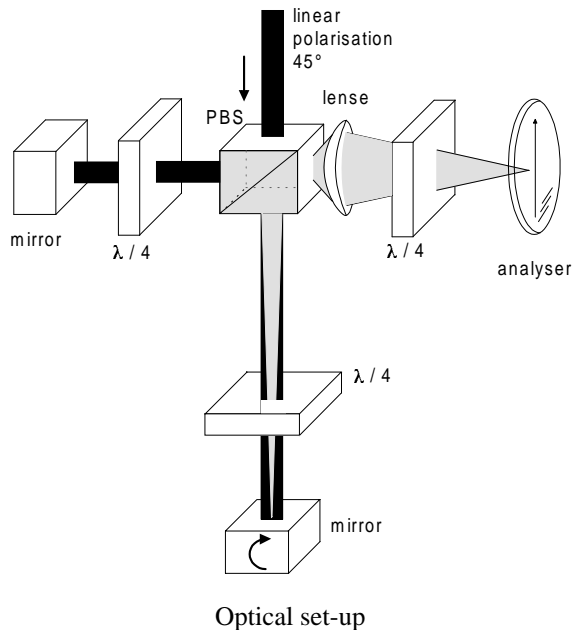
In our approach the pattern can be shifted with high accuracy and, most importantly, the shift is independent of the wavelength  $\lambda$ . The polarization optical elements are needed to achieve the wavelength independent shift of the fringe pattern. The  $\lambda/4$ -plate in the output path generates two circularly polarized fields with opposite rotation resulting in a linearly polarized field. The direction of polarization is determined by the phase difference between the circularly polarized fields. By tilting one mirror a space variant phase difference is realized, leading to a space variant orientation of the linearly polarized field [8].

The analyzer projects the field onto a particular polarization orientation generating a fringe pattern. Rotating the analyzer by an angle  $\alpha$  results in a phase shift of the pattern by  $\varphi = \frac{\alpha}{2}$ . In contrast to piezo-driven phase shifting devices, this approach demands substantially less accuracy for a phase shifting unit: A phase shift of  $\varphi = 2\pi \cdot x$  is realized by the rotation of an analyzer by  $\alpha = \frac{x}{\pi}$  which is to be compared to a mechanical shift of a mirror by  $\delta z = \lambda \cdot \frac{x}{2}$ .

The obtained phase shift is independent of wavelength, since it is only proportional to the rotation angle of the analyzer. The realisation of the phase shift can also be described by a topological phase change on the Poincaré-sphere (Berry / Pancharatnam-Phase) which is another explanation for wavelength independence [10]. For multiple wavelength applications one can use multiple light sources, which may be mutually incoherent. Different wavelengths result in different periods and initial phases of the fringe pattern. The scene may be observed by multiple detectors, e.g. a 3-chip color CCD, equipped with appropriate filters for each wavelength channel. Thus, parallel fringe evaluation for obtaining absolute data is possible.

#### References

- [8] K.-H. Brenner, S. Sinzinger, "Polarization coded images realized with binary phase masks", Ann. Rep., Angewandten Optik, Erlangen p. 26 (1988).
- [10] U. Krackhardt, K.-H. Brenner, "The Berry-Phase applied to optical Metrology", Verh. der DPG KY 5.3, ISSN 0420-0195 (1999).
- [13] U. Krackhardt, K.-H. Brenner, "Flächenhaftes Interferometer", patent pending, IPC G01B 9/02 (1998)



## 4 Refractive Volume Holograms realized by Ion Exchange in Glass

U.W. Krackhardt, J. Bähr

Beam deflection, shaping and focussing are the basic operations needed in any optical processing system. Typically, these operations are realized by micro-optical components based on diffraction or refraction. The properties of an ideal micro-optical component are design flexibility, optimum optical performance, durability and ease of assembly. Optimum optical performance is determined by energy efficiency, minimum aberrations and application specific wavelength dependence properties.

We intend to use refractive volume holograms (RVH) as a basic concept for achieving micro-optical components with high efficiency, high durability, simple assembly behaviour, low wavelength dependence and high design flexibility. Especially the wavelength sensitivity is reduced in RVHs since the restriction of the phase to the interval  $[-\pi, \pi]$  is omitted.

RVHs show a distribution of refractive index within the *volume* in contrast to surface structures like conventional computer generated holograms (CGH) or classical refractive optical elements like lenses or prisms. As a consequence, the surface of these elements is flat and thus accessible for further processing like structuring, coating or assembly. In contrast to diffractive (Bragg effect) volume holograms, RVHs are refractive and therefore show substantially less wavelength dependence and high efficiency even for small deflection angles.

We realize RVHs by ion exchange in glass. A schematic process flow is depicted in fig. 1: Starting from a desired index distribution an appropriate diffusion mask is calculated. The mask is optimized in terms of positions and areas of openings. To this end, continuous index values are mapped to the binary mask structure by half-toning. In a thermal diffusion process silver ions penetrate the glass surface at the locations of the openings and replace the sodium ions in the glass matrix. The area of an opening defines the amount of silver ions and thus the increase of refractive index in that region. After removing the mask layer a component with space-variant refraction in the volume is obtained.

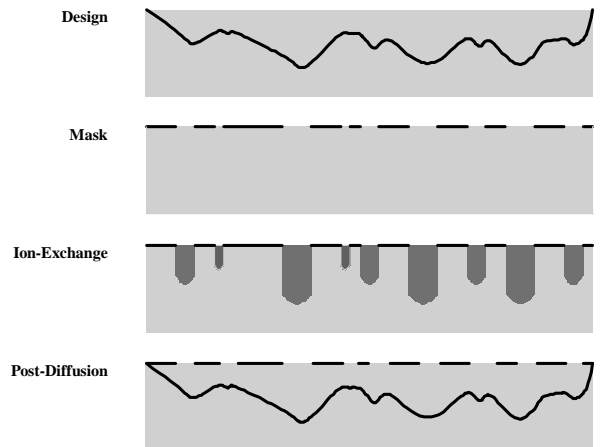


**Fig. 1** Schematic process flow for realizing an RVH

However, the thermal diffusion process is non-linear and isotropic, which implies two requirements for the mask geometry: i) The area of an opening is not proportional to the index change. ii) Mask openings must not be mutually separated by more than the diffusion length in order to obtain smooth index distributions. We incorporate these requirements into the fabrication process by i) process characterization specific for a substrate material and ii) applying an appropriate precompensation in the half-tone matrix [12]

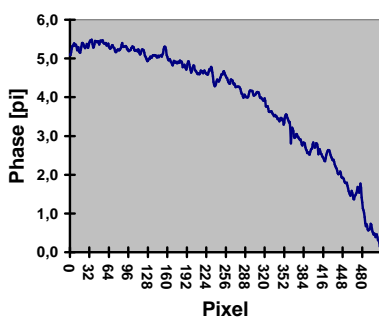


**Fig. 2** Phase ramp without compensation

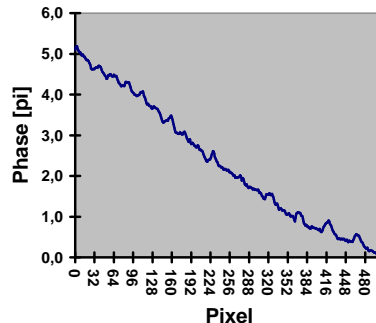


**Fig. 3** Phase ramp with compensation, no post-diffusion

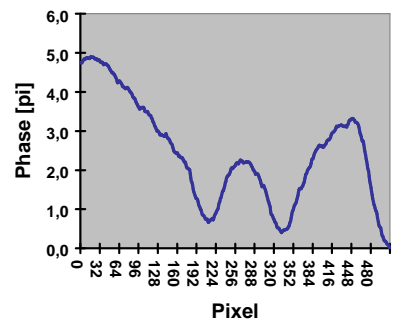


**Fig. 4** Phase profile of a 9-fold beam-splitter implemented as a RVH

## References

- [12] U. Krackhardt, J. Bähr, K.-H. Brenner, "Herstellung von Strahlteilern mit kontinuierlicher Phase durch Ionen-Austausch", DGaO Tagung, Bad Nenndorf (1998).

## 5 Analysis of phase anomalies and design of continuous phase elements

*Karl-Heinz Brenner*

The design of diffractive optical elements is typically performed by iterative Fourier transform algorithms like the Gerchberg-Saxton-Algorithm. In the image plane, a desired intensity distribution is enforced, whereas in the element plane the fabrication requirements are implemented. For phase elements, e.g., the amplitude is set to unity and the phase is adjusted freely. In the case of phase elements realized by ion exchange, an additional requirement has to be met: the phase distribution has to be continuous. This requirement is due to the fact that for the ion exchange process, the index distribution arises from thermal diffusion of Ag-Ions. Thus the gradient of the index distribution cannot exceed typical values of  $2\pi/8\mu m^{-1}$ . According to the iterative Fourier transform algorithm, there are two sources of discontinuities. Regular discontinuities originate from the fact that the phase is a  $2\pi$ -periodic function.

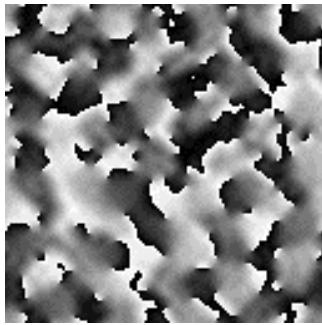


Fig. 1 Anomalous phase distribution

These discontinuities can be removed simply by continuation, which is a process of adding multiples of  $2\pi$  until all phase steps have vanished. The second kind of discontinuities are phase anomalies as shown in fig. 1. These anomalies are a serious problem, since they appear frequently and prevent a phase distribution from being continuable. This can be realized by observing in fig. 1 that some of the edge lines of the discontinuities do not form a closed region. A first attempt to solve this problem was treated in [5] for one-dimensional or two-dimensional but x-y-separable distributions and for non-separable distributions in [2] with moderate success.

The new approach is also based on the iterative Fourier transform algorithm but it starts in the element plane with a height distribution instead of a phase distribution. After each iteration the height  $h$  is corrected according to

$$h^{n+1}(x, y) = h^n(x, y) + \varphi^{n+1}(x, y) - 2\pi \cdot \text{SAW}\left(\frac{h^n(x, y)}{2\pi}\right)$$

where the SAW-function is a modulo-function which maps its argument to values between -0.5 and 0.5. As a second step, a low-pass filter is applied to the height distribution to assure that the height gradient does not exceed a maximum value. Fig. 2 shows the resulting height distribution for a binary  $256^2$ -image as desired intensity (fig. 3). The phase corresponding to this height varies over  $4\pi$  and is guaranteed to be continuable. The digital reconstruction shown in fig. 3 has a standard deviation of 10 % after 300 iterations.

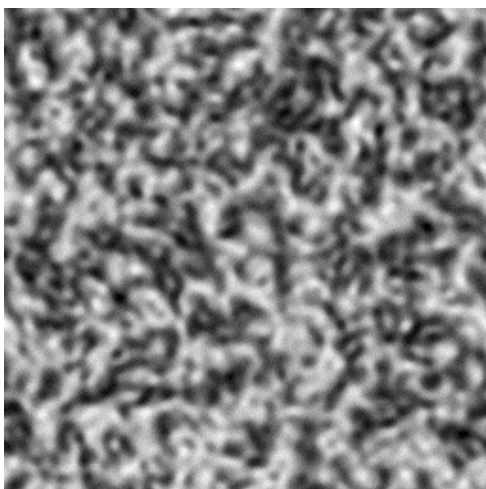


Fig. 2 Continuous height distribution

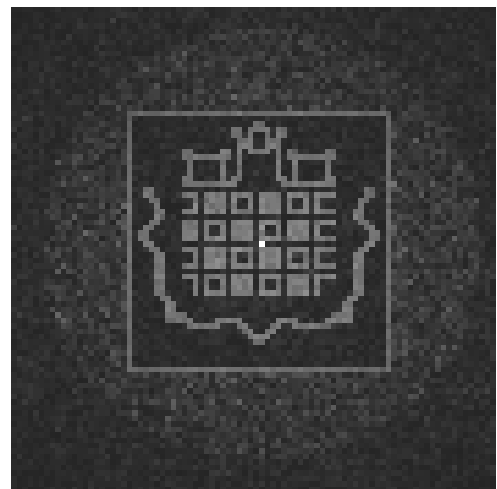


Fig. 3 Reconstructed intensity from the phase of fig. 2

The continuous height distribution can be transferred to a binary diffusion mask by half-toning, resulting in a RVH, as described on page 5 of this report.

## References

- [2] D. Birk, „Entwurf und Analyse kontinuierlicher optischer Phasenelemente“, Diplomarbeit Lehrstuhl für Angewandte Optik, Universität Erlangen 1994
- [5] M.T. Gale, „Continuous relief optical elements for two-dimensional array generation“, Appl. Optics 31,14 pages 2526 (1993)

## 6 Realization of planar microlenses with long focal distance by mask-synthesis

J. Bähr, K.-H. Brenner

We report a realization of microlenses with a diameter of  $400 \mu\text{m}$  and a focal distance of  $17\text{mm}$  with diffraction limited performance. Applications of these lenses are in the field of sensors, such as in a Hartman-Shack system or in confocal microscopy.

For fabrication we exclusively use thermal ion exchange in glass, since the parameters of this process are quite easy to control. By combining different mask structures a broad variety of phase distributions can be realized. Examples include astigmatic or aspherical lenses. In our present work we use a synthesis of concentric ring apertures to attain microlenses with a wavefront optimized for collimating/focussing purposes. The minimum feature size is  $2 \mu\text{m}$ , which is given by the photolithographic and the wet-etch process applied for mask structuring. The optimum structure of the mask is determined by numerical simulation of the diffusion process. For simulation we use the k-model [7] for non-linear diffusion problems implemented in cylindrical coordinates. Figure 1 shows a photograph of a mask consisting of circular rings typical for our process. Figure 2 shows the phase distribution of an element after an ion exchange process of 460 minutes at a temperature of  $400^\circ\text{C}$ . The solid line represents the phase distribution through the center of the element measured in a transmission interferometer, the dotted line shows the simulated data. Figure 2 indicate the good agreement between experiment and simulated data. To smoothen the index distribution we applied an additional post heating step [1]. Figure 3 shows the index distribution and the simulation result after a post heating time of 300 minutes at  $400^\circ\text{C}$ . The shape of the wavefront is in sufficient approximation hyperbolic, which is ideal for focussing/collimating applications. The focal distance is  $17\text{mm}$ , which corresponds to a numerical aperture of 0.012. Figure 4 shows the wave aberrations of the microlens compared to simulated data. According to the Maréchal criterion the lens provides diffraction limited performance within its whole aperture. By the use of different optimized mask structures a variety of focal distances can be achieved on one single substrate. Applying the fabrication parameters mentioned above, the focal length can be adjusted to values between  $10\text{mm}$  and  $30\text{mm}$ , which corresponds to a numerical aperture of 0.02 to 0.007. By variation of the time of ion exchange numerical apertures up to 0.05 can be realized with this technique.

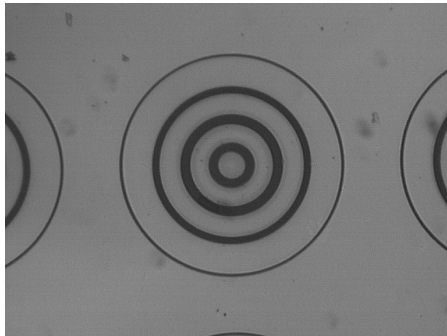


Fig. 1 Photo of a mask structure etched in a Titanium layer

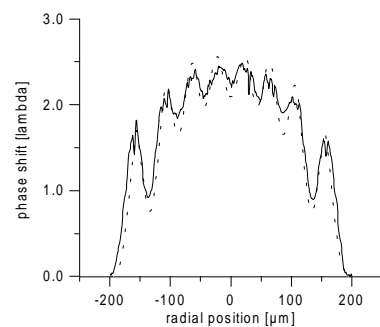


Fig. 2 Index distribution after the ion exchange process

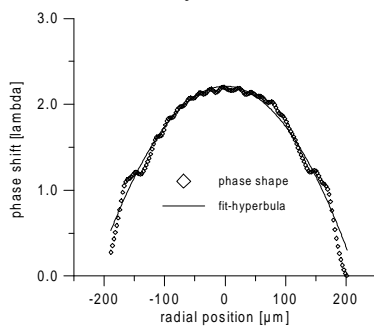


Fig. 3 Index distribution after the post heating step and fit hyperbola

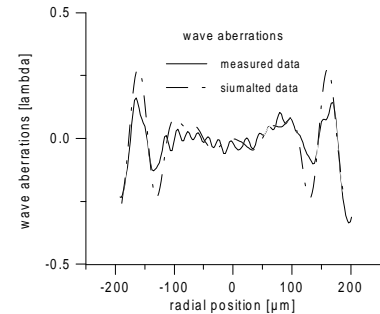


Fig. 4 Wave aberrations of the optimized microlens

## References

- [1] J. Bähr and K.-H. Brenner. Realization and optimization of planar refracting microlenses by Ag-Na ion-exchange techniques. *Applied Optics*, 35:5102–5107, 1996.
- [7] K. Iga, M. Oikawa, S. Misawa, J. Banno, and Y. Kokubun. Stacked planar optics: an application of the planar microlens. *Appl. Opt.*, 21:3456–3460, 1982.

## 7 1:3 Beam-Splitting with a H-ROD Element

J. Bähr, K.-H. Brenner

We report a realization of a 1:3 beam-splitting operation using a H-ROD element. Since the reflection at the surface virtually completes the H-ROD to a full-cylindrical ROD lens, the H-ROD performs telecentrical imaging with the full numerical aperture [3]. A test pattern consisting of point sources was imaged over a half-pitch distance. On the surface of the H-ROD, which is a filter-plane [3] we deposited a special amplitude grating in reflection mode to provide that light of the 1., -1. and 0. order of the input pattern is preserved in the element. At the end plane of the H-ROD the duplicated images could be obtained. Figure 1 shows a schematic setup.

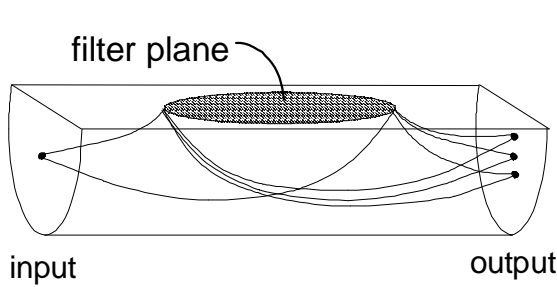


Fig. 1 Schematic setup of the 1:3 beam shaper



Fig. 2 Simulation of the splitting operation using the BPM method

Figure 2 shows a simulation of the filter operation with the beam propagation method. The orientation of the H-ROD element is analog to that in fig. 1, the thin white line marks the interface between the element and the air. The amplitude grating was calculated holographically.

For experimental realization we used a half-pitch H-ROD element fabricated in a SCHOTT BGG 31 substrate glass with a refractive index of 1.474. The index was increased in the center by an amount of  $\Delta n = 0.065$  by the field assisted silver-sodium ion exchange. The diameter of the element was  $740 \mu\text{m}$ , the half-pitch length was  $3900 \mu\text{m}$ . The filter grating was deposited on the surface of the H-ROD element. Matching the grating with an optical glue, which has a higher refractive index compared with that of the H-ROD surface, enables that light can travel out of the element at certain points of the surface. For demonstration we used a three-point test pattern. Figure 3 shows the point to point imaging of the test pattern without the filter. Figure 4 demonstrates the result of the filter operation.



Fig. 3 Image of the test pattern without filtering

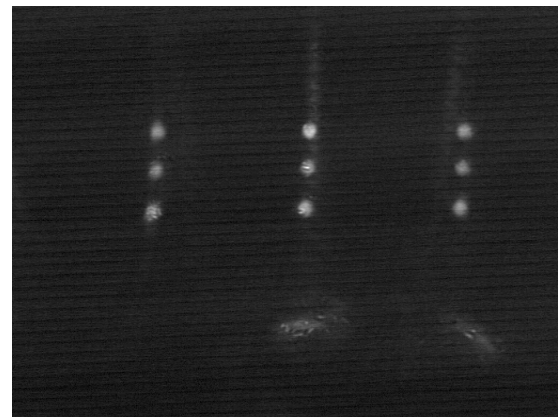


Fig. 4 Result of the filter operation

## References

- [3] D. Dragoman, K.-H. Brenner, M. Dragoman, J. Bähr, and U. Krackhardt. Hemispherical-rod microlens as a variant fractional fourier transformer. *Optics Letters*, 23:1499–1501, 1998.

## 8 Variable Fractional Fourier Transform using an H-Rod Microlens

D. Dragoman, K.-H. Brenner, M. Dragoman, J. Bähr, U. Krackhardt

The fractional Fourier transform, widely used for signal processing and characterization applications, is a linear integral transform of a field distribution characterized by a degree of fractionality  $\alpha$ . We have microoptically implemented [3] a fractional Fourier transformer which simultaneously displays a range of continuously varying  $\alpha$  values. The device which performs this task is a semicylinder graded-index medium with a radial distribution of the refractive index in a direction transverse to the cylinder axis,

$$n(x, y) = n_0 \left( 1 - \frac{A^2}{2} (x^2 + y^2) \right) \quad x \leq 0$$

called H-rod microlens (Fig.1a). Typical values are  $n_0 = 1.544$ ,  $A = 1.2 \cdot 10^{-3} \mu\text{m}^{-1}$  and  $500 \mu\text{m}$  for the diameter of the H-rod microlens.

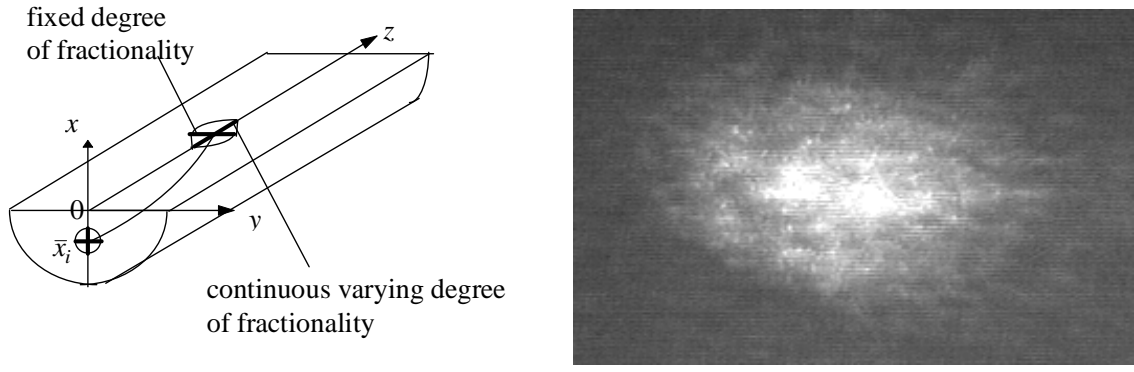


Fig.1 (a) The off-axis illuminated H-rod microlens and (b) the recorded output when illuminated with a monomode optical fiber

If illuminated off-axis the H-rod microlens displays on its plane surface the fractional Fourier transform of the incident light with variable  $\alpha$  values in the meridional plane and the fractional Fourier transform with constant  $\alpha$  value in the sagittal plane. Along the  $z$  direction, the degree of fractionality  $\alpha$  recorded at a distance  $z = \alpha\pi/2A$  is determined by the excitation position  $\bar{x}_i$  and excitation angle  $\bar{p}_i$  as

$$\tan\left(\alpha\frac{\pi}{2}\right) = -n_0 A \frac{\bar{x}_i}{\bar{p}_i}$$

The range of displayed  $\alpha$  values depends on the angular divergence of the incident light beam and its point of incidence on the H-rod microlens. A span of  $\alpha$  values from 0.5 to 1.5 is easily obtainable. Fig.1b presents the intensity recorded on the plane surface of the H-rod if illuminated with a monomode optical fiber. In this case the output should have a Gaussian envelope determined both by the width of the incident beam and the  $\bar{x}_i, \bar{p}_i$  parameters. The experimental results confirm the shape of the envelope as well as its width dependencies. Possible applications of the variable fractional Fourier transformer include optical tomography as a method of reconstructing the phase space distribution of the incident light from fractional Fourier transforms with various  $\alpha$ -values.

## References

- [3] D. Dragoman, K.-H. Brenner, M. Dragoman, J. Bähr, U. Krackhardt, „Hemispherical-rod microlens as a variant fractional Fourier transformer“, Optics Letters 23, 1499-1501 (1998)

## 9 Experimental Characterization of Microoptical Objects in Phase Space

D. Dragoman, M. Dragoman, J. Bähr, K.-H. Brenner

Using an optical set-up which allows the optimization of blurring and a magnification of the object (Fig.1), we have measured for the first time the spectrogram of individual microlenses with sub-mm diameters [4]. The angular and spatial variables (phase space variables) of the spectrogram are related to the coordinates in the output plane by

$$p = -\frac{x_{out}}{f} \quad \text{and} \quad x = \frac{f_0 \sin \theta}{f \cos \theta} y_{out}$$

respectively where  $\theta$  is the angle made by the rotated slit with the  $x$  axis.

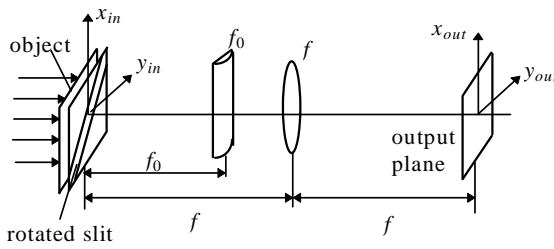


Fig.1 Experimental set-up

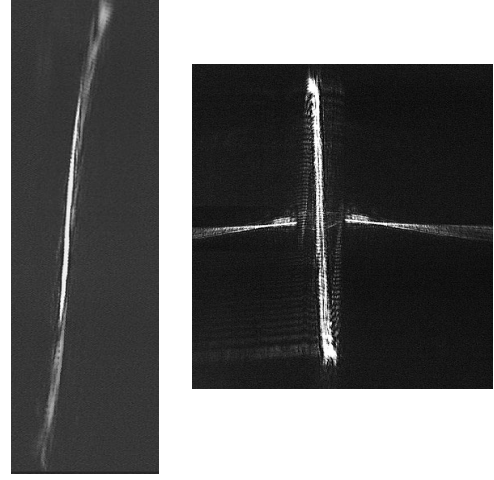


Fig.2 Experimental results

Fig.2a shows the spectrogram of an individual microlens from a microlens array, with a diameter of about 250  $\mu\text{m}$  and Fig.2b is the spectrogram of a GRIN-lens with a 1 mm diameter; both objects were illuminated with a plane wave. For purely phase objects, characterized by a transmission function  $T(x) = \exp(i\phi(x))$ , the phase space image (spectrogram) is given by  $\delta(kp - \partial\phi/\partial x)$  with  $k$  the wavenumber of light. In the case of quadratic phase objects, for example ideal lenses, this phase space image should be a straight line. From the slope  $\tan \Phi$  of the spectrogram one can then determine the focal length  $F$  of the microlens as  $F = f_0 \tan \theta \tan \Phi$  as well as the eventual aberrations identified as deviations from the straight line. The measurements were found to be in very good agreement with those obtained from experimental interferometric results of the same objects. Typical values for the focal lengths of the spherical and cylindrical lenses are  $f = 300$  mm and  $f_0 = 200$  mm. The importance of phase space measurements is that they offer an optimum display of information of the studied object. Our results show that phase space measurements of microoptical objects can be performed with a sufficient accuracy.

## References

- [4] D. Dragoman, M. Dragoman, J. Bähr, K.-H. Brenner, „Phase space measurements of micro-optical objects“ , Applied Optics, submitted

## 10 Angular Multiplexing for optical Board to Board Interconnections

R.Klug, U. W. Krackhardt and K.-H.Brenner

Optical signal transmission benefits, among other features, from its huge bandwidth, which is exploited commonly by wavelength, time or space division multiplexing (WDM, TDM, SDM). As optical interconnections becoming attractive also for short distances, a further alternative, angle division multiplexing (ADM) is now applicable. Over distances in the order of 10 meters, the coupling angle  $\vartheta$  between the symmetry axis of a step-index multimode fiber and the principle propagation direction of a beam is conserved [6] as depicted in figure 1. This conservation behavior can be used for coding different channels for multiplexed transmission. To exploit conservation of coupling angle for multiplexed transmission lines, suitable optical set-ups for multiplexing and de-multiplexing (DeMUX) operations were designed and a particular DeMUX device was tested.

When an off-axis Gaussian beam is launched into a multi-mode fiber, the intensity in the farfield of the fiber is distributed over an annular ring with the radius corresponding to the coupling angle  $\vartheta$ . The finite thickness of the circle results from three effects:

1. Finite angular spectrum (finite  $\vec{k}$ -spectrum) of the input beam.
2. Due to the uncertainty principle the finite core diameter  $d$  of the fiber core results in an angular spread  $\lambda/d$  (where  $\lambda$  is the wavelength) at the fiber outlet.
3.  $\vartheta$ -blur due to fiber interaction: Imperfections of both the fiber core and the core/cladding interface induce mode coupling, described by a mode coupling constant  $D$  [6]. Since this effect scales with the propagation distance, angular blur increases with the fiber length  $L$ .

The maximum number  $N$  of multiplexed channels is basically limited by the number of modes in the fiber. However, cross-talk requirements may reduce this number due to mode-coupling leading to  $\vartheta$ -blur. Therefore there are the fiber length  $L$ , the core diameter  $d$ , the fiber NA and the mode-coupling constant  $D$  to optimize the transmission line for a maximum degree of multiplexing.

The DeMUX device maps light distributed over different annular rings (corresponding to different  $\vartheta$ -directions) to separated points in the detector plane. The device consists of two lenses that image the fiber output to a detector plane and a filter to perform the mapping between annular rings and positons on the detector plane. Basically, this filter acts as a set of prisms of different orientations and deflection angles, each clipped by an annular ring. Within each ring the deflection angle is constant and tuned to match the corresponding detector position. Figure 2 shows a setup where the detectors are lined-up.

Because of design flexibility in the first step we used a computer generated diffractive element (CGH). To achieve high diffraction efficiency  $\eta$  and low stray light (i.e. low cross-talk) an 8-level CGH with  $\eta \approx 80\%$  can be fabricated using lithography and reactive ion etching (RIE). Such a deflecting component can be designed for almost arbitrary detector geometries. It is even possible to include fan-out operations.

With a binary amplitude CGH and a step-index multimode fiber with a core diameter  $d = 200\mu\text{m}$ , an NA=0.48 and a length  $L = 0.4$  m we could demultiplex 11 channels with an average cross-talk of -11 dB [9]. A higher number of multiplexed channels or lower cross-talk requires the use of fibers with higher NA or shorter length or smaller coupling constant D.

## References

- [6] G. Glode, Optical Power Flow in Multimode Fibers, Bell Syst. Techn. J. **51**, 1767-83 (1972)
- [9] R. Klug, U. W. Krackhardt, K.-H. Brenner, Directional Multiplexing for optical Board to Board Interconnections, Proc. SPIE 3573, p. 174-77 (1998)

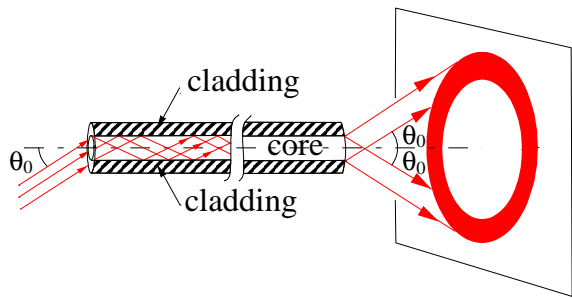


Figure 1: Conservation of coupling angle  $\vartheta$

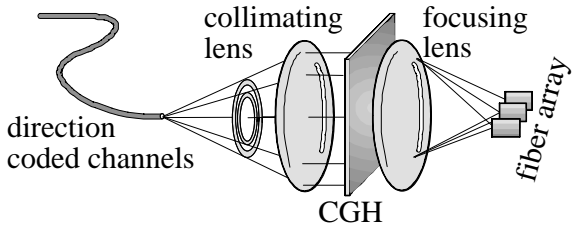


Figure 2: Concept for a DeMUX device

## 11 Microobjectives with large numerical aperture by stacking of microlenses

*R.Klug, J. Bähr and K.-H.Brenner*

In the field of microoptics there is a demand for objectives with large numerical aperture (NA). Examples include objectives for optical disks or highly light efficient collimating optics. If one wants to use microlenses in these applications, the NA of a single microlens is not sufficient. Consequently an objective should be build.

For constant radius of curvature the NA of a classical lens can be increased by increasing the refractive index of the glass. In order to avoid aberrations, aspherical surfaces are required. For Gradient index (GRIN) microlenses the maximum NA is determined by the index difference between exchanged and nonexchanged regions. These types of lenses have many advantages over classical lenses. Most importantly, the index distribution is inside the glass, allowing an optimization of the index profile [1] and leaving the substrate surfaces flat. Therefore several layers of micro lenses can be stacked without an air interface, realizing a large NA multi-lens imaging system. An additional benefit of stacking several lenses is the possibility to correct for different types of aberrations. Thereby large aperture systems can be corrected also for large fields, which would be difficult or impossible for a single lens system.

We have already demonstrated earlier [11], that it is possible to design and fabricate a stacked optical systems with microlenses, when we realized an off-axis confocal sensor head with a NA of 0.32. Now we realized an on-axis 16x32 array of microobjectives with a  $NA = 0.45$  from three GRIN-lens arrays.

For the optical design a previously developed a GRIN-ray trace software(TraceSys) [see annual report 1997] was used. Figure 1 shows the light propagation through the stack as calculated by TraceSys. For the design, we used lenses, which were available and were corrected for light collimation, having a diffraction limited  $NA$  of 0.15.

The microobjective, constructed from 3 lenses was designed for a two to one demagnification task at a wavelength of  $0.63\mu m$ . The imaging result for test masks is shown in figure 2. The  $NA$  of the objective was determined with the equation:

$$NA = \frac{0.61\lambda}{x_{min}}$$

where  $\lambda$  is the wavelength and  $x_{min}$  is the resolved linewidth.

The microobjective resolves structures of  $2.4\mu m$  size. This corresponds to a  $NA$  of 0.3 at the image side of the microobjective and a  $NA$  of 0.15 at the object side respectively. Thus the objective has an overall power of 0.45, which is three times larger than a single microlens. The fabrication of microobjectives with larger  $NA$  is possible by stacking several lens layers. Additionally the aberrations of the objective can be corrected either by optimizing the gradient index profile of individual microlenses or by optimizing the system design. For future work, a combined optimization of gradient index profile and system geometry will be included in the trace software.

## References

- [1] J. Bähr, K.-H. Brenner, Realization and optimization of planar microlenses by Ag-Na ion exchange techniques, Appl. Opt. 35, 5102-7 (1996)
- [11] R. Klug, K.-H. Brenner, A. Knüttel, Microoptic implementation of an array of 1024 confocal sensors, Proceedings of the 3rd Int. Cong. and Exh. on Optoelectr., Opt. Sens. and Meas. Techn. p. 155-60 (1998)

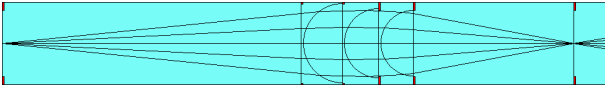


Figure 1: Raytrace of a microobjective from 3 GRIN lenses

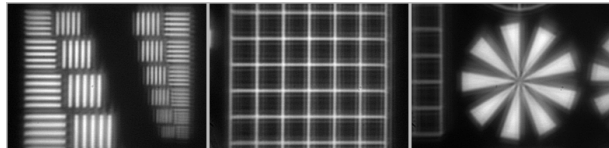


Figure 2: 2 to 1 imaging, linewidth in the object plane is  $3.175\mu m$

## 12 Software Tools for Pattern Design in Lithography

U.W. Krackhardt, O. Döringer

In lithography there are different pattern description languages mostly optimized for the need of microelectronics. Except for very expensive professional software there is no assistance for interactive design or previewing of patterns. We decided to create software tools running under MS-Windows<sup>TM</sup> for our in-house laser lithograph:

**Previewer:** A tool to inspect at designed patterns before they are converted or plotted. This saves a considerable amount of time in the design process.

**Expander:** Helps to extend common pattern description languages by adding customer specific commands. This is useful when using special objects like circles, beziér curves, specially styled labels, etc. The customer specific dialect is then mapped to the standard commands of an appropriate pattern description language.

**Texter:** This tool allows plotting standard text fonts of a MS-Windows-System by means of a lithograph. The user has the same freedom in choosing font, style, size as in common WISIWYG-text editors. The *texter* maps the text as a bitmap graphic onto a user selected standard pattern description language.

**Designer:** Putting all the other tools together and adding a visual drawing pane naturally leads to a design software. The main difference of this tool as compared to standard design software under MS-WINDOWS is that geometric parameters can be determined with high resolution. As an example, consider a lithograph with 200 nm address grid writing on 4“ substrates. This means that coordinates range from 0 to 500.000, approximately. The Metafile- format in MS-WINDOWS encodes coordinates by 16-bit values allowing only 65.535 steps.

Currently, only the previewer is in a ready-to-use state. The other tools are in a beta-version-state. The previewer is capable of handling huge files since only the visible portion of a pattern file is loaded and evaluated. The user can interactively select a zoom window with adjustable zoom factor and position within the complete pattern. If provided by the pattern description language the user can select particular layers of a pattern to be displayed. Additionally, pattern information is displayed like bounding box, number of call statements, number of ignored commands, etc. In case of errors while interpreting the file, the error messages are listed with details. By double clicking an error message an external editor can be invoked which supports line addressing to display the line causing the error.

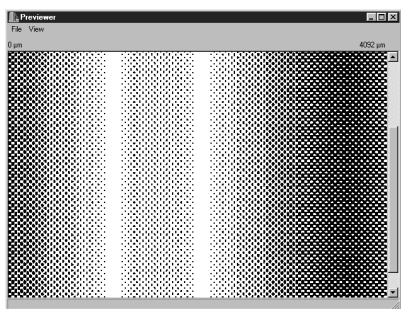


**Fig. 1:** Main window showing a half-tone mask for the fabrication of a beam splitter with continuous phase by ion-exchange

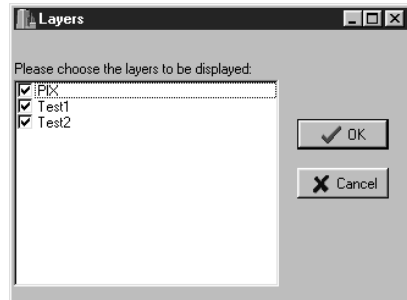


**Fig. 2:** Layer-select dialog

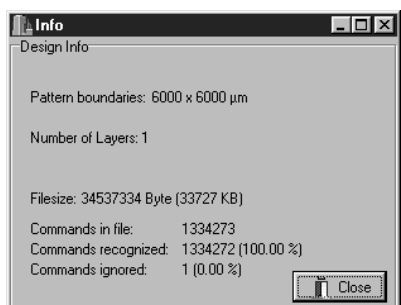


**Fig. 3:** Pattern information dialog

Error report			
	Line	Error Code	Error Description
	3	2	Parameters expected.
	4	5	Wrong parameter recognized.

**Fig. 4:** Section of an error message

## 13 Software for Computer Aided Surface Profiling

*U.W. Krackhardt, T. Schmelcher, S. Schiek*

Surface profiling is a contact method for sensing profiles of flat surfaces. In our department we use an alpha-step stylus prober for characterization of micro-optical elements. We have developed a software for remote control of the stylus prober and for real-time data acquisition. The data is evaluated for process control.

Thus, etch rates of a reactive ion etching facility (RIE) or the volume change due to ion exchange in glass can be characterized. The prober is calibrated by interferometric testing of glass sheets having a square wave surface profile realized by RIE.

The alpha-step profiler is originally designed for manual operation. We modified the built-in electronic controller to enable remote control. Thus, a user can interact with the prober by a PC. Data is acquired by means of a ADC-card and is displayed on-line on the screen. The software can easily be set to the different configurations of the prober: Scan speed and depth resolution can be adjusted for metric display of scanning results.

There are two operating modes of the software:

**Manual mode:** The software continuously acquires data from the prober. The user can manually control the prober. This mode is to provide a comfortable visual prober interface as an extension of the standard print out on a paper strip. The user can easily find the region of interest and a proper setup for scan speed and depth resolution.

**Automatic mode:** As soon as the user starts a scan by pushing a button of the prober, data acquisition is triggered. To this end the control signal of the stepper motor of the prober is continuously monitored. Since scan speed and depth resolution are known by set-up, the scan depth is displayed as a function of relative lateral co-ordinates.

As the software is generally suited for acquiring time dependent voltage signals, thus acting as a PC based oscilloscope, we call it *TimeScan*.

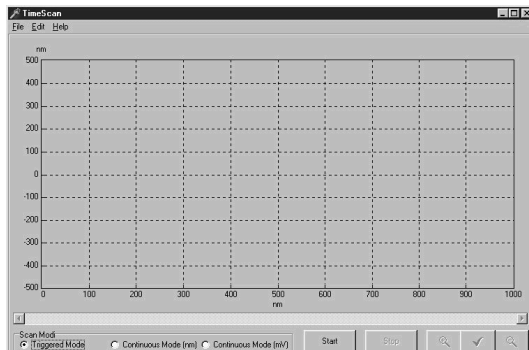


**Fig. 1** Main window

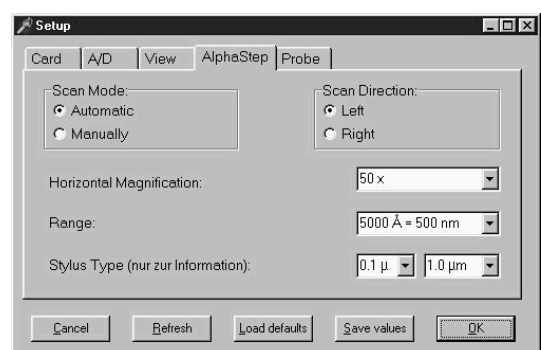


**Fig. 2** Parameter dialog for interaction with the alpha-step stylus prober

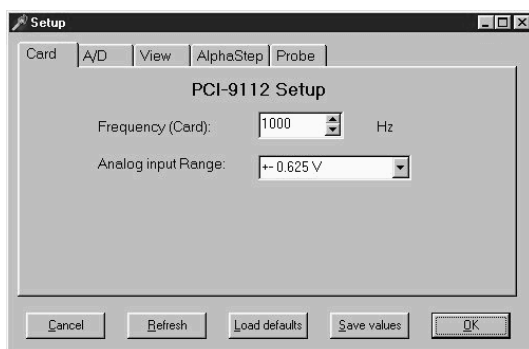


**Fig. 3** Dialog for setting up the ADC

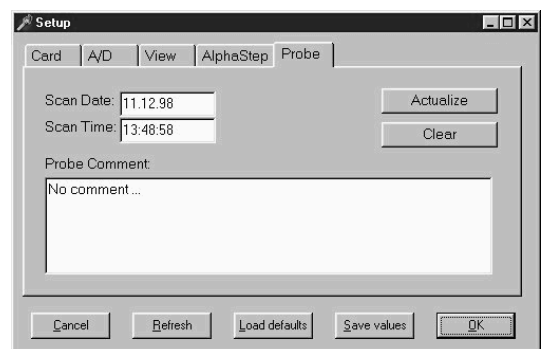


**Fig. 4** Dialog for entering session info

## A List of recent Publications

- [1] J. Bähr and K.-H. Brenner. Realization and optimization of planar refracting microlenses by Ag-Na ion-exchange techniques. *Applied Optics*, 35:5102–5107, 1996.
- [2] D. Dragoman, K.-H. Brenner, M. Dragoman, J. Bähr, and U. Krackhardt. Hemispherical-rod microlens as a variant fractional Fourier transformer. *Otics Letters*, 23:1499–1501, 1998.
- [3] R. Klug, U. W. Krackhardt, and K.-H. Brenner. Directional multiplexing for optical board to board interconnections. *Proc. SPIE 3573*, pages 174–177, 1998.
- [4] A. Knüttel R. Klug, K.-H. Brenner. Microoptic implementation of an array of 1024 confocal sensors. *Proceedings of the 3rd Int. Cong. and Exh. on Optoelectr., Opt. Sens. and Meas. Techn.*, pages 155–60, 1998.
- [5] K.-H. Brenner U. Krackhardt. Flächenhaftes Interferometer. patent pending, IPC G01B 9/02, 1998.
- [6] K.-H. Brenner U. Krackhardt, J. Bähr. Herstellung von Strahlteilern mit kontinuierlicher Phase durch Ionenaustausch, 1998. DGaO Tagung, Bad Nenndorf.
- [7] U. Krackhardt and K.-H. Brenner. The berry-phase applied to optical metrology. In *Verh. der DPG*, page KY 5.3, 1999. ISSN 0420-0195.
- [8] D. Dragoman, M. Dragoman, J. Bähr, and K.-H. Brenner. Phase space measurements of micro-optical objects. *Applied Optics*, submitted.
- [9] K.-H. Brenner, Hossam ElGindy, Hartmut Schmeck, Heiko Schröder Dynamically Reconfigurable Architectures. *Dagstuhl-Seminar-Report 201*. No.98081 1998,page 9.
- [10] K.-H. Brenner, U. Krackhardt. Komponenten und Aufbautechniken für mikro-optische Systeme zur Informationsübertragung und -verarbeitung. *it+ti* submitted.
- [11] R. Klug, U. Krackhardt, K.-H. Brenner. Richtungsmultiplex für optische Verbindungen zwischen Platinen. Tagungsbeitrag ORT 98 Paderborn.

Publisher: Lehrstuhl für Optoelektronik  
Fakultät für Mathematik und Informatik  
Universität Mannheim  
B6, 26  
D–68131 Mannheim  
Germany

Tel: +49 621 292–5459  
Fax: +49 621 292–1605  
Mail: info@oe.ti.uni-mannheim.de  
WWW: <http://www.ti.uni-mannheim.de/~oe>

Editor: Thilo Schmelcher

Tel: +49 621 292–5541  
Mail: t.schmelcher@oe.ti.uni-mannheim.de

Print: Universitätsdruckerei Mannheim